Russian Physics Journal, Vol. 43, No. 6, 2000

SOLID-STATE PHYSICS

ROLE OF POINT DEFECTS IN MARTENSITIC TRANSFORMATIONS

V. V. Kulagina* and E. F. Dudarev

UDC 539.2

The effect of point-defect complexes on martensitic phase transformations in a bcc system with low elastic moduli is studied by means of computer simulation. The interaction of strain fields generated by defects is shown to facilitate realization of a martensitic transition from the bcc to fcc or ω-like structure depending on the defect symmetry.

At present, much consideration is being given to structural transformations and instability of the crystal lattice as the point of martensitic transition is approached. An understanding of the physics of phenomena occurring in the premartensitic region is intimately connected with the mechanism responsible for the nucleation of the martensite phase and the role of structural imperfections in this process.

According to the effects of structural defects on martensitic transformations, the latter may be arbitrarily classified in two groups: strong first-order transitions, on the one hand, and "weak" first-order transitions and those approaching their second-order cousins, on the other [1, 2]. The first group comprises different types of steel and the majority of iron-based alloys where the nucleation of the martensite phase occurs at the sites of complex structural defects like grain boundaries, interfaces, free surface, etc. Being local stress concentrators, defects of this kind lower the activation barrier for the martensite-phase nucleation. Among the materials undergoing a "weak" first-order transition or a near-second-order transition are In–Tl alloys based on noble metals, TiNi, etc. Alloys belonging to this group exhibit marked pretransition anomalies. These show up in abnormal behavior of electrical resistance and softening of shear moduli and phonon frequencies, diffuse scattering, superlattice reflections seen in X-ray and electron diffraction patterns, and a change in the electron spectrum [3–10].

For weak first-order transitions, the driving force of transformation is known to be lower by severalfold than that found in the strong first-order transitions. In this case, there is reason to believe that simple crystal defects (dislocations, stacking faults, point-defect complexes, etc.) and their interaction with soft phonon modes play an important part in the nucleation of the martensite phase. The defects may be nucleation or pinning centers for regions with a short-range order of atomic displacements and intermediate shear structures.

The characteristics of martensitic transformations depend greatly on the alloying-element concentration and prior thermal history, which bears witness to the profound influence of point defects on martensitic transformations. For instance, when a small amount of a third alloying element is added to TiNi, a martensitic transformation to the rhombohedral *R*-phase takes place. To account for the detailed X-ray diffraction pattern of superlattice reflections observed in TiNi(Fe) prior to transformation, it was suggested in [11, 12] that the low dip in the $TA_2<\xi\xi 0>$ phonon branch gives rise to modulated lattice relaxation in the neighborhood of defects (in this case, iron atoms may appear as defects). As the temperature is lowered, the modulated lattice-relaxation regions increase in size and interact to provide a certain mutual orientation. At a certain temperature, a stable martensite nucleus is formed. In [13], it is noted that in TiNi(Fe) alloys, the type of microstructural distortions around iron atoms, the occurence of which is treated as formation of short-range order displacements, depends on the composition of the alloy. With a low iron concentration, distortions following the pattern seen in the ω-phase take place around iron impurity atoms under soft-lattice conditions. This leads to the $B2 \rightarrow R$ transition as the temperature goes down.

Of importance in this case is not only the presence of defects but their distribution in the high-temperature phase as well. It is well known that in Ni – rich TiNi alloys, the transformation sequence varies according to the prior thermal history from $B2 \rightarrow B19'$ in quenched alloys to $B2 \rightarrow R \rightarrow B19'$ in annealed alloys ($B19'$ is a monoclinic martensite). This fact is presumably attributable to the development of elastic-stress fields of rhombohedral type as Ni_4Ti_3 particles are precipitated, or excess nickel atoms at titanium sublattice sites in annealed alloys are ordered [14]. There are other experimental data

Siberian Physicotechnical Institute at Tomsk State University. *Siberian State Medical University. Translated from Izvestiya Vysshikh Uchebnykh Zavedenii, Fizika, No. 6, pp. 58–63, June, 2000. Original article submitted July 5, 1999.

1064-8887/00/4306-0493$25.00

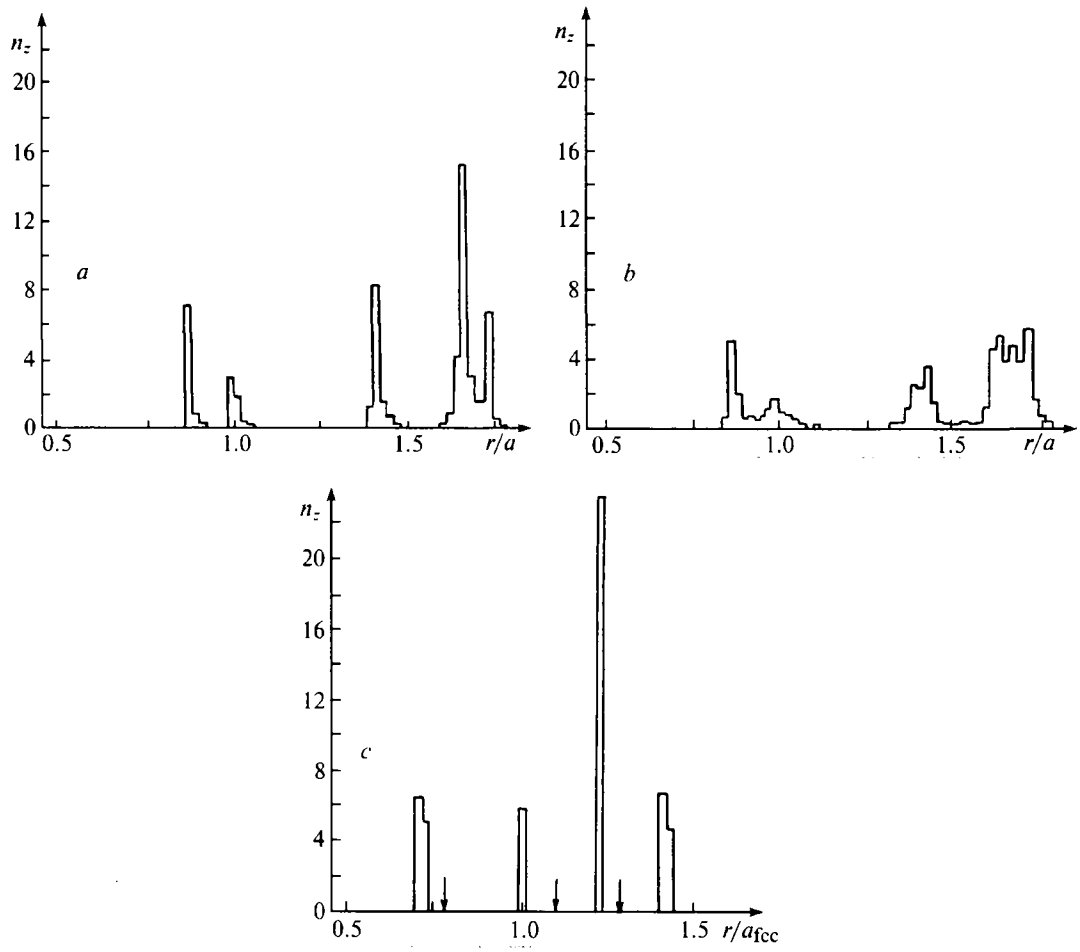

Fig. 1. Distribution of the number of atomic neighbors by the nearest-neighbor distance.

indicative of realization of martensitic phase transformations when structural defects like vacancies [15] or substitutional atoms [16, 17] are ordered.

In this work, we investigate the role of point defects in realization of martensitic transformations in a bcc system. The defects to be considered are complexes of vacancies of varying symmetry. The calculations are performed by the molecular-dynamics methods following Parrinello and Rahman who allowed for changes in the volume and shape of the model block [18, 19]. For describing the interatomic interaction, use is made of an empirical potential of the form [20]

$$\varphi(r) = \begin{cases} \dfrac{A_n}{r^n} + A_0 + A_1 r + A_2 r^2 + A_3 r^3 + A_m r^m, & r < r_c, \\ 0, \quad r \geq r_c, \end{cases}$$

where r_c is the potential truncation radius chosen between the third and forth coordination spheres. The parameters of the potential are found from preassigned values of the binding energy, elastic moduli, and lattice constant. The calculations are performed for the bcc lattice with high and low elastic moduli ("stiff" and "soft" lattices, respectively) [20].

The model block is taken to be a cube of size $n \times n \times n$, where n is the edge of the block in terms of the crystal-lattice parameter. The values of n vary between 3 and 8. Periodic boundary conditions are imposed. In a system with high elastic moduli, displacements in the vicinity of a defect are localized. In a soft lattice, the distortions around the defect may reach the computational-cell boundary, and the defect cannot be regarded as being isolated. In this case, the use of periodic boundary conditions is equivalent to examination of an infinite defect-superlattice with primitive translation vectors equal to the edges

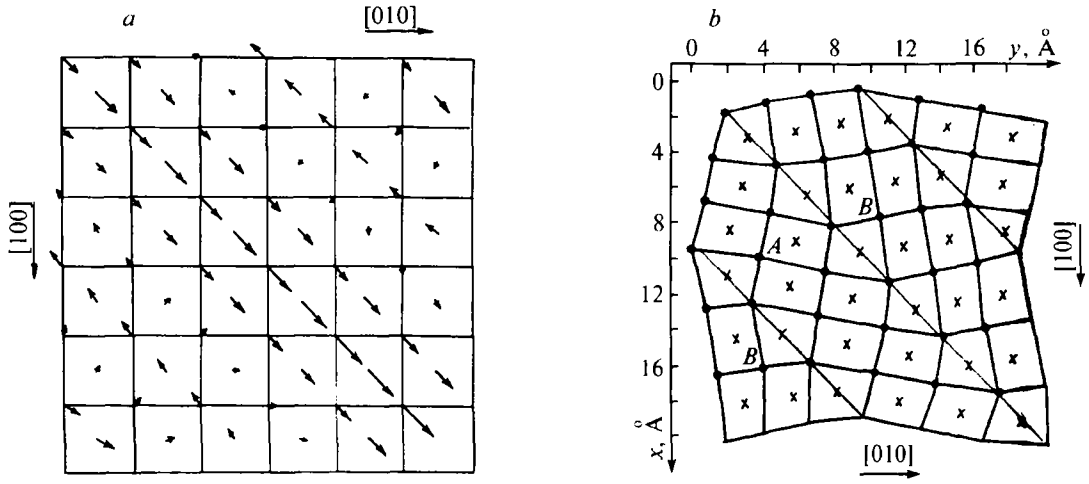

Fig. 2. Schematic sketch of atomic displacements from the parent bcc-lattice sites (*a*) and projections of atoms on the {001} plane (*b*).

of the computational cell. The use of periodic boundary conditions places certain constraints on computer simulation of martensitic transformations, imposing synchronism on the processes occurring in all primitive cells of the superlattice.

In the calculations with a potential corresponding to a high-modulus lattice, the bcc structure is stable for any type of defect and any size of the calculation block. Under low-modulus conditions, wherein the system is in the vicinity of the stability limit, both the defect symmetry and the size of the model block (the latter specifies the defect concentration) appear to be of significance. The interaction of regularly-arranged vacancies with the displacement-field symmetry corresponding to the parent-structure symmetry stabilizes the latter. The interaction of displacement fields of tetragonal symmetry that occurs around pairs of vacancies at a distance of the second-nearest neighbors toward the <001> bcc lattice initiates a transition to the fcc structure by the homogeneous Bain deformation mechanism for $n = 5$. In this case, the bcc→fcc transformation occurs by 9% contraction along the <100> and <010> directions and by 28% expansion along the <001> axis of the bcc lattice.

For a clear illustration of transformation of one structure to another (or lack of it), histograms of distribution of n_i number of atomic neighbors by distance are calculated. In the absence of transformation, the relaxation-induced atomic displacements in the vicinity of the defect do no more than smear the histogram peaks. The positions of maxima remain unchanged and correspond to atomic spacings found in the parent bcc structure. If the system undergoes a structural transformation, positions of histogram peaks will change accordingly. As an example, Fig. 1 shows histograms obtained in calculating relaxation near a divacancy for $n = 5$ in a lattice with high elastic moduli (Fig. 1*a*) and with low moduli before (Fig. 1*b*) and after (Fig. 1*c*) transformation. As evident from the histograms, the lattice with low elastic moduli exhibits significant static atomic-displacements in the vicinity of the defect. The histogram in Fig. 1*c* testifies that the bcc→fcc transition has taken place. This is supported both by the relative positions of the histogram peaks corresponding to the atomic spacings $a\sqrt{2}/2$, a, $a\sqrt{1.5}$, $a\sqrt{2}$, ... of the fcc lattice and by the area under the peaks which is proportional to the coordination numbers of the fcc structure (12, 6, 24, 12, ...). The distinct peaks of the fcc lattice suggest that the atomic displacements in the vicinity of the defect are localized in the product structure.

The low elastic modulus C' is characteristic of low shear strength of the $\{1\bar{1}0\}$ planes along the <110> direction. In this connection, we have examined defects located in planes of this type and beyond the planes. The calculations show that the defects in the $\{1\bar{1}0\}$ plane responsible for significant atomic displacements in this plane contribute to the bcc-lattice instability and martensitic bcc→fcc transformation. The transition occurs by shuffle displacements of the $\{1\bar{1}0\}$ plane along the <110> direction accompanied by the lattice strain through the Bain deformation mechanism.

As an illustration, we refer to calculation results shown in Fig. 2 for a defect in the shape of a triangle of trivacancies in the $\{1\bar{1}0\}$ plane for $n = 6$. The direction and magnitude of displacements of the $\{1\bar{1}0\}$ planes are shown by arrows in Fig. 2*a*, and the projections of all atoms of the model block on the {001} plane are depicted in Fig. 2*b*. The projections of atoms located in two neighboring {001} planes of the parent bcc-lattice are marked by crosses and full circles. The defect is located in the {110} plane passing through the center of the computational cell. As can be seen from the figure, the regular

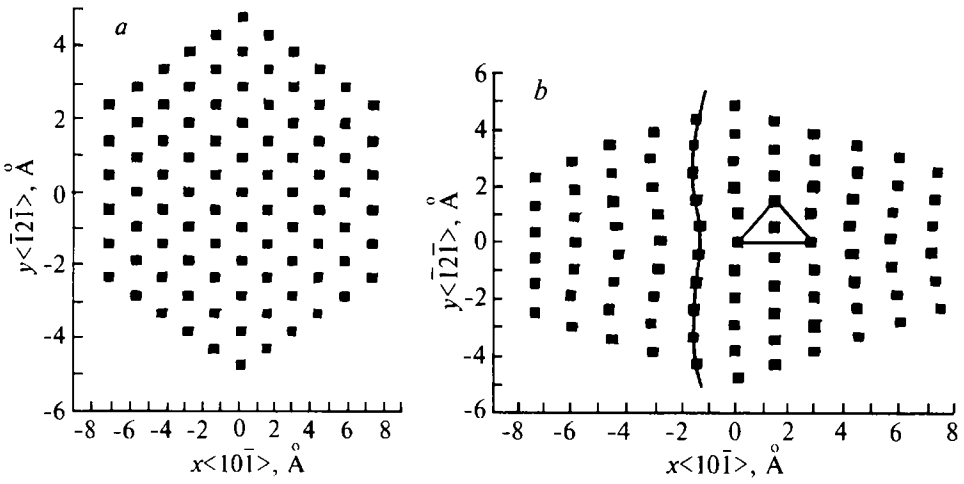

Fig. 3. Projections of atoms on the {111} plane in the parent state (*a*) and upon relaxation (*b*). The triangle represents the position of the defect.

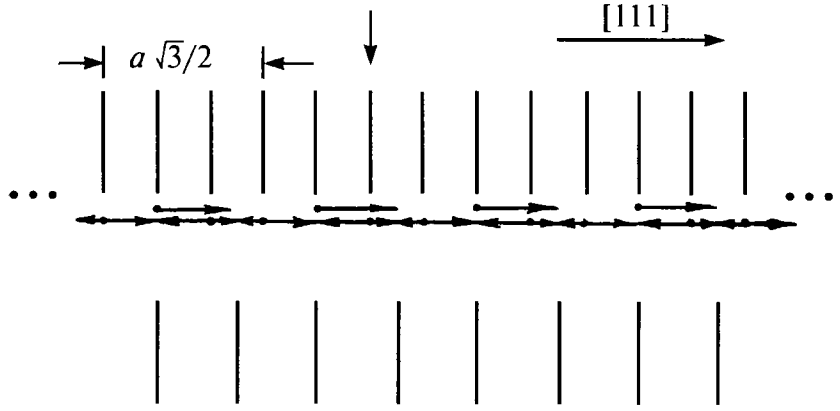

Fig. 4. Schematic sketch of displacements of {111} atom chains upon formation of the ω-like structure. Vertical lines demonstrate positions of the {111} planes before (at the top) and after (at the bottom) the transformation.

arrangement of the {001}planes is not changed by the transition. The product structure has twinning elements. Orientation relationships between the bcc and fcc lattices in the region between twin boundaries will differ. In the regions labeled *A* in Fig. 2*b*, the lattice is observed to extend along the <010> axis and contract along the <100> and <001> axes of the parent bcc lattice. In regions *B*, on the contrary, the lattice extends along the <100> axis and contracts along the <010> and <001> axes. The histogram displays satellite peaks, attributed to shuffle displacements of the $\{1\,\bar{1}\,0\}$ planes, in addition to the principal maxima typical for the fcc lattice.

Defects lying outside planes of the $\{1\,\bar{1}\,0\}$ type prevent shuffle displacements of these planes and hinder the bcc→fcc transition. In this case, as the lattice instability builds up, it is not improbable that the martensitic transformation will occur by another mechanism. Thus relaxational atomic displacements due to defects in the form of vacancies lying in the {111} plane initiate a transition from the bcc structure to the ω-like structure. To determine the principal directions of atomic displacements, we have examined projections of atoms in the model block on different planes. Figure 3 shows projections of atoms on the {111} plane in the parent bcc-lattice (*a*) and after the transition (*b*). A comparison of Figs. 3*a* and *b* suggests that no appreciable atomic displacements occur in the {111} defect plane, since the projection pattern is, on the whole, retained. However, pronounced atomic displacements do take place in the $\{\bar{1}\,2\,\bar{1}\}$ planes along the $\{10\,\bar{1}\}$ direction. The fact that the atomic displacements are of wave nature merits notice. The displacement waves propagate as far as the model block boundaries and hence are due to the interaction of spatially regular defects. The boundary conditions do not prevent the

displacement transfer from one spacing cell to another. Thus, it follows from Fig. 3*b* that a long-period structure is formed. An analysis of projections of atoms on the $\{10\bar{1}\}$ and $\{\bar{1}2\bar{1}\}$ planes show that displacements of the <111> atom chains from opposite directions cause the $\{111\}$ planes to split. The displacements of the <111> atom chains along the <111> direction follow the scheme shown in Fig. 4. At the top of the figure are the positions of the $\{111\}$ planes in the parent bcc-lattice, and at the bottom are their positions upon relaxation. The arrow pointing downwards represents the defect plane. The arrows pointing sidewards show the direction and magnitude of displacements of atom chains. Eventually, two planes of the product structure are formed from three $\{111\}$ planes of the bcc structure, as is the case in the ω-transformation. The $\{111\}$ planes are split, and atoms from different planes are concentrated into one plane following the scheme shown in Fig. 4.

On the basis of the results obtained in this work, we conclude that the presence of structural defects in a lattice with low elastic moduli, their symmetry, concentration, and interaction may be essential factors affecting realization of martensitic transformation. Defects retaining the fcc-lattice symmetry stabilize the lattice, while those breaking the symmetry of the parent structure may contribute to its instability and favor martensitic transformation. Defects responsible for considerable displacements in the $\{1\bar{1}0\}$ planes are shown to initiate the martensitic bcc→fcc transformation. The latter represents shuffle displacements in the $\{1\bar{1}0\}$ planes along the <110> direction accompanied by the Bain deformation of the lattice. The atomic displacement fields in the vicinity of defects lying outside planes of the $\{1\bar{1}0\}$ type prevent the $\{1\bar{1}0\}$ <110> shuffle displacements and hinder the martensitic bcc→fcc transformation by this mechanism. In this case, an alternative pathway for the development of martensitic transformation is not ruled out. The interaction of defects lying in the $\{111\}$ planes gives rise to a long-period ω-like structure formed by shuffle displacements of the <111> atom chains.

Even though the investigations under review have been performed on complexes of vacancies, we believe that the conclusions arrived at are of a more general character and are valid for the case where atoms of an alloying element are considered instead of vacancies.

REFERENCES

1. L. E. Tanner and M. Wuttig, Mater. Sci. Eng. A, **127**, No. 2, 137–144 (1990).
2. J. A. Krumhansl and Y. Yamada, Mater. Sci. Eng. A, **127**, No. 2, 167–181 (1990).
3. A. I. Lotkov and A. V. Kuznetsov, Fiz. Met. Metalloved., **66**, No. 5, 903–909 (1988).
4. O. Mercier, N. Melion, G. Greemafud, and J. Hagi, J. Appl. Phys., **51**, No. 3, 1833–1834 (1980).
5. T. M. Brill, S. Mittelbach, W. Asmus, *et al.*, J. Phys.: Condens. Matter, **3**, 9621–9627 (1991).
6. V. N. Khachin, S. A. Muslov, V. G. Pushin, and V. V. Kondratyev, Metallofizika, **10**, No. 1, 102–104 (1988).
7. P. Moine, J. Allain, and B. Renker, J. Phys. F: Metal Phys., **14**, 2517–2523 (1984).
8. H. Fietze, M. Mullner, and B. Renker, J. Phys. C: Solid-State Phys., **17**, L529–L532 (1984).
9. S. K. Satya, S. M. Shapiro, M. B. Salamon, and C. M. Wayman, Phys. Rev. B, **29**, No. 11, 6031–6035 (1984).
10. T. Ohba, S. M. Shapiro, S. Aoki, and K. Otsuka, J. Appl. Phys., **33**, L1631–L1633 (1994).
11. Y. Yamada, Y. Noda, M. Takimoto, and K. Furukawa, J. Phys. Soc. Japan, **54**, No. 8, 2940–2947 (1985).
12. Y. Yamada, Met. Trans. A., **19**, No. 4, 777–781 (1988).
13. S. V. Anokhin, V. N. Grishkov, and A. I. Lotkov, Metallofizika, **11**, No. 5, 44–48 (1989).
14. A. I. Lotkov, V. N. Khachin, and V. N. Grishkov, in: Physical Mechanics and Computer-Aided Design of Materials, Vol. 2 [in Russian], Nauka, Novosibirsk (1995), pp. 202–213.
15. Liu Ping and J. L. Dunlop, J. Mater. Sci., **23**, No. 4, 1419–1424 (1988).
16. A. A. Arkhangelskaya, V. S. Litvinov, and V. V. Poleva, Fiz. Met. Metalloved., **48**, No. 6, 1256–1261 (1979).
17. V. S. Litvinov and A. A. Arkhangelskaya, Thermal Treatment and Physics of Metals [in Russian], Urals Research Center of the Russian Academy of Sciences, Sverdlovsk (1982).
18. M. Parrinello and A. Rahman, J. Appl. Phys., **52**, No. 12, 7182–7187 (1981).
19. A. Rahman, Mater. Sci. Forum, 1, 211–222 (1984).
20. V. V. Kulagina, "Simulation of Martensitic Transformations in BCC Materials with Defects," Paper No. 3641, Deposited at VINITI, Moscow (December 11, 1998).